

Facile Synthesis of Monodisperse Microspheres and Gigantic Hollow Shells of Mesoporous Silica in Mixed Water–Ethanol Solvents

Huijuan Zhang, Jun Wu, Longping Zhou, Dayong Zhang, and Limin Qi*

Beijing National Laboratory for Molecular Sciences (BNLMS), State Key Laboratory for Structural Chemistry of Unstable and Stable Species, College of Chemistry, Peking University, Beijing 100871, P. R. China

Received August 30, 2006. In Final Form: November 12, 2006

Mesoporous silica materials with a variety of morphologies, such as monodisperse microspheres, gigantic hollow structures comprising a thin shell with a hole, and gigantic hollow structures consisting of an outer thin shell and an inner layer composed of many small spheres, have been readily synthesized in mixed water–ethanol solvents at room temperature using cetyltrimethylammonium bromide (CTAB) as the template. The obtained mesoporous silica generally shows a disordered mesostructure with typical average pore sizes ranging from 3.1 to 3.8 nm. The effects of the water-to-ethanol volume ratio (r), the volume content of tetraethyl orthosilicate TEOS (x), and the CTAB concentration in the solution on the final morphology of the mesoporous silica products have been investigated. The growth process of gigantic hollow shells of mesoporous silica through templating emulsion droplets of TEOS in mixed water–ethanol solution has been monitored directly with optical microscopy. Generally, the morphology of mesoporous silica can be regulated from microspheres through gigantic hollow structures composed of small spheres to gigantic hollow structures with a thin shell by increasing the water-to-ethanol volume ratio, increasing the TEOS volume content, or decreasing the CTAB concentration. A plausible mechanism for the morphological regulation of mesoporous silica by adjusting various experimental parameters has been put forward by considering the existing state of the unhydrolyzed and partially hydrolyzed TEOS in the synthesis system.

Introduction

The synthesis of mesoporous silica materials with controlled structures and morphologies is attracting increasing attention both for their widespread potential applications and as a result of a fundamental interest in biomineralization processes (e.g., biosilicification in diatom).^{1–4} For example, much attention has been paid to the synthesis of well-defined mesoporous silica spheres since spheres are very promising for applications in chromatography, catalysis, cosmetics, and photonic crystals.^{5–16} It is noted that monodisperse mesoporous silica spheres have been prepared by various synthetic routes; however, there are only a few reports on the solution synthesis of monodisperse

mesoporous silica spheres with micrometer-sized diameters.¹³ On the other hand, many recent efforts have been devoted to the controlled synthesis of mesoporous silica spheres with hollow interiors due to their potential applications in drug delivery, controlled release, enzyme immobilization, biomolecule separation, confined-space catalysis, as well as acoustic, thermal, and electrical insulation.^{17–32} In this regard, a variety of spherical templates, such as polymer latex particles,¹⁷ emulsions,^{18–25} vesicles,^{26–28} and polymer aggregates,²⁹ have been employed in combination with surfactant templates for the dual-templating fabrication of hollow mesoporous silica spheres, while some other synthetic techniques, including acoustic cavitation,³⁰ have also been applied. In particular, emulsion droplets have turned

* Corresponding author. E-mail: liminqi@pku.edu.cn.

- (1) Soler-Illia, G.; Sanchez, C.; Lebeau, B.; Patarin, J. *Chem. Rev.* **2002**, *102*, 4093.
- (2) Stein, A. *Adv. Mater.* **2003**, *15*, 763.
- (3) Berggren, A.; Palmqvist, A. E. C.; Holmberg, K. *Soft Matter* **2005**, *1*, 219.
- (4) (a) Vrieling, E. G.; Sun, Q.; Beelen, T. P. M.; Hazelaar, S.; Gieskes, W. W. C.; van Santen, R. A.; Sommerdijk, N. A. J. M. *J. Nanosci. Nanotechnol.* **2005**, *5*, 68. (b) Botterhuis, N. E.; Sun, Q.; Magusin, P. C. M.; van Santen, R. A.; Sommerdijk, N. A. J. M. *Chem.—Eur. J.* **2006**, *12*, 1448.
- (5) Huo, Q.; Feng, J.; Schuth, F.; Stucky, G. D. *Chem. Mater.* **1997**, *9*, 14.
- (6) Grun, M.; Lauer, I.; Unger, K. K. *Adv. Mater.* **1997**, *9*, 254.
- (7) Qi, L.; Ma, J.; Cheng, H.; Zhao, Z. *Chem. Mater.* **1998**, *10*, 1623.
- (8) Boissiere, C.; Kummel, M.; Persin, M.; Larbot, A.; Prouzet, E. *Adv. Funct. Mater.* **2001**, *11*, 129.
- (9) (a) Kosuge, K.; Singh, P. S. *Chem. Mater.* **2001**, *13*, 2476. (b) Kosuge, K.; Murakami, T.; Kikukawa, N.; Takemori, M. *Chem. Mater.* **2003**, *15*, 3184. (c) Kosuge, K.; Kikukawa, N.; Takemori, M. *Chem. Mater.* **2004**, *16*, 4181.
- (10) Rao, G. V. R.; Lopez, G. P.; Bravo, J.; Pham, H.; Datye, A. K.; Xu, H. F.; Ward, T. L. *Adv. Mater.* **2002**, *14*, 1301.
- (11) Nooney, R. I.; Thirunavukkarasu, D.; Chen, Y.; Josephs, R.; Ostafin, A. E. *Chem. Mater.* **2002**, *14*, 4721.
- (12) Ma, Y.; Qi, L.; Ma, J.; Wu, Y.; Liu, O.; Cheng, H. *Colloids Surf., A* **2003**, *229*, 1.
- (13) Yano, K.; Fukushima, Y. *J. Mater. Chem.* **2004**, *14*, 1579.
- (14) Yamada, Y.; Nakamura, T.; Ishi, M.; Yano, K. *Langmuir* **2006**, *22*, 2444.
- (15) Yang, L. M.; Wang, Y. J.; Sun, Y. W.; Luo, G. S.; Dai, Y. Y. *J. Colloid Interface Sci.* **2006**, *299*, 823.
- (16) Wang, L.; Qi, T.; Zhang, Y.; Chu, J. *Microporous Mesoporous Mater.* **2006**, *91*, 156.

- (17) Tan, B.; Rankin, S. E. *Langmuir* **2005**, *21*, 8180.
- (18) Fowler, C. E.; Khushalani, D.; Mann, S. *Chem. Commun.* **2001**, 2028.
- (19) Li, W.; Sha, X.; Dong, W.; Wang, Z. *Chem. Commun.* **2002**, 2434.
- (20) (a) Li, Y.; Shi, J.; Hua, Z.; Chen, H.; Ruan, M.; Yan, D. *Nano Lett.* **2003**, *3*, 609. (b) Zhu, Y.; Shi, J.; Shen, W.; Dong, X.; Feng, J.; Ruan, M.; Li, Y. *Angew. Chem., Int. Ed.* **2005**, *44*, 5083.
- (21) Sun, Q.; Kooyman, P. J.; Grossmann, J. G.; Bomans, P. H. H.; Frederik, P. M.; Magusin, P. C. M. M.; Beelen, T. P. M.; van Santen, R. A.; Sommerdijk, N. A. J. M. *Adv. Mater.* **2003**, *15*, 1097.
- (22) Sun, Q.; Magusin, P. C. M. M.; Mezari, B.; Panine, P.; van Santen, R. A.; Sommerdijk, N. A. J. M. *J. Mater. Chem.* **2005**, *15*, 256.
- (23) (a) Wang, J.; Xia, Y.; Wang, W.; Mokaya, R.; Poliakoff, M. *Chem. Commun.* **2005**, 210. (b) Wang, J.; Xia, Y.; Wang, W.; Poliakoff, M.; Mokaya, R. *J. Mater. Chem.* **2006**, *16*, 1751.
- (24) Fujiwara, M.; Shiokawa, K.; Tanaka, Y.; Nakahara, Y. *Chem. Mater.* **2004**, *16*, 5420.
- (25) Li, W.; Coppens, M.-O. *Chem. Mater.* **2005**, *17*, 2241.
- (26) Tan, B.; Lehmler, H.-J.; Vyas, S. M.; Knutson, B. L.; Rankin, S. E. *Adv. Mater.* **2005**, *17*, 2368.
- (27) Yeh, Y.-Q.; Chen, B.-C.; Lin, H.-P.; Tang, C.-Y. *Langmuir* **2006**, *22*, 6.
- (28) Djojoputro, H.; Zhou, X. F.; Qiao, L. Z.; Yu, C. Z.; Lu, G. Q. *J. Am. Chem. Soc.* **2006**, *128*, 6320.
- (29) (a) Zhu, Y.; Shi, J.; Chen, H.; Shen, W.; Dong, X. *Microporous Mesoporous Mater.* **2005**, *84*, 218. (b) Zhu, Y.; Shi, J.; Shen, W.; Chen, H.; Dong, X.; Ruan, M. *Nanotechnology* **2005**, *16*, 2633.
- (30) Rana, R. K.; Mastai, Y.; Gedanken, A. *Adv. Mater.* **2002**, *14*, 1414.
- (31) Lin, H.-P.; Mou, C.-Y.; Liu, S.-B.; Tang, C.-Y. *Chem. Commun.* **2001**, 1970.
- (32) Han, S.; Hou, W.; Xu, J.; Li, Z. *Colloid Polym. Sci.* **2004**, *282*, 1286.

out to be very effective templates for the templating of hollow mesoporous silica spheres of different sizes and structures; examples include water-in-oil,¹⁹ oil-in-water,^{20–22} supercritical CO₂-in-water,²³ water-oil-water,²⁴ and oil-water-oil²⁵ emulsion systems. It is noteworthy that gigantic hollow silica spheres composed of primary mesoporous silica spheres were prepared from an EO₇₆PO₂₉EO₇₆/butanol/ethanol/water quaternary emulsion system recently.²² Nevertheless, it remains a challenge to explore facile emulsion templating routes toward hollow mesoporous silica spheres with tailored structures and morphologies. Furthermore, it is worthwhile to develop a unified solution method to selectively synthesize well-defined, solid and hollow spheres/shells of mesoporous silica by simply adjusting the synthesis parameters.

The synthesis of monodisperse silica spheres was first described by Stöber et al. in 1968, employing a water-alcohol-ammonia-tetraalkoxysilane system.³³ The Stöber silica particles obtained were microporous with low specific surface area and pore volume.³⁴ Stöber's procedure was modified through introducing cationic surfactants into the synthesis system to fabricate submicrometer-sized mesoporous silica spheres with high surface area.⁶ Recently, monodisperse, submicrometer-sized, mesoporous silica spheres with highly ordered hexagonal regularity were obtained by employing a water-methanol-sodium hydroxide-tetramethoxysilane (TMOS)-alkyltrimethylammonium chloride system.¹³ We found that the Stöber's procedure could be further modified to fabricate both monodisperse mesoporous silica spheres and hollow mesoporous silica shells by using cetyltrimethylammonium bromide (CTAB) as the template under appropriate composition conditions. Herein, we report the facile synthesis of monodisperse microspheres and gigantic hollow shells of mesoporous silica through the ammonia-catalyzed hydrolysis of tetraethyl orthosilicate (TEOS) in mixed water-ethanol solutions of CTAB at room temperature. It has been revealed that the morphology of the obtained mesoporous silica materials can be readily adjusted by simply changing the composition parameters such as the water-to-ethanol volume ratio (r), the volume content of TEOS (x), and the CTAB concentration in the solution.

Experimental Section

Synthesis. The synthesis of mesoporous silica products was simply achieved by the ammonia-catalyzed hydrolysis of TEOS in mixed water-ethanol solvents using CTAB as the template at room temperature. Typically, 0.5 mL of CTAB solution (0.04 M), 0.5 mL of ammonia solution (1.25 wt %), and 0.9 mL of water were first mixed with 2.0 mL of ethanol, which was followed by the addition of 0.3 mL of TEOS under vigorous stirring, giving a water-to-ethanol volume ratio (r) of 0.95 and a TEOS volume content (x) of 0.07. After ~10 s of stirring, the mixture was allowed to stand under static conditions at room temperature for 3 h, leading to the formation of a white precipitate. The resultant products were collected by centrifugation, washed with water, dried at 40 °C overnight, and calcined in air at 550 °C for 6 h. In the experiments, the synthesis parameters including the r value, the x value, and the CTAB concentration were varied in order to systematically adjust the morphology of the obtained mesoporous silica products.

Characterization. Scanning electron microscopy (SEM) images were recorded using an FEI STRATA DB235 microscope at 10 kV or an AMARY 1910FE microscope at 5 kV. Transmission electron microscopy (TEM) images were taken on a JEOL JEM-200CX microscope operating at 160 kV. Optical microscopy (OM) images were recorded on a Nikon ECLIPSE E600 microscope. Powder

X-ray diffraction (XRD) was performed using a Rigaku Dmax-2000 with Cu K α radiation. Nitrogen adsorption-desorption measurements were performed using Micromeritics ASAP 2010. The pore size distribution was calculated from the adsorption isotherm curves using the Brunauer-Joyner-Halenda (BJH) method.³⁵

Results and Discussion

Effect of the Water-to-Ethanol Volume Ratio (r). Figure 1 shows representative SEM and TEM images of the mesoporous silica products obtained at a CTAB concentration of 4.8 mM and a TEOS volume content of 0.07. As shown in Figure 1a,b, monodisperse, well-defined silica microspheres with an average diameter of 1.22 μm (standard deviation ~ 3.9%) were produced when the water-to-ethanol volume ratio was $r = 0.63$. Our preliminary TEM observation revealed that these microspheres were actually solid spheres rather than hollow spheres. The small-angle XRD pattern exhibits a weak diffraction peak corresponding to a d spacing of ~4.0 nm (Figure S1a, Supporting Information), indicating the presence of disordered mesopores in the silica microspheres. The nitrogen adsorption-desorption isotherms of the silica spheres are of type IV and display a clear hysteresis loop (Figure 2a), which is characteristic of mesoporous materials with cage-like or disordered pores.^{23,35} These silica spheres have a BET surface area of 485 m² g⁻¹ and a pore volume of 0.375 cm³ g⁻¹. The pore size distribution determined from the adsorption branch shows a sharp peak at 2.3 nm together with two small peaks located between 8 and 14 nm, and the average pore size was calculated to be 3.1 nm. These results suggest that the obtained silica spheres are actually monodisperse mesoporous silica microspheres with a disordered mesostructure. It is noted that the monodisperse mesoporous silica spheres obtained at room temperature in the water-methanol-sodium hydroxide-TMOS-cetyltrimethylammonium chloride system showed a highly ordered hexagonal regularity and high surface area (larger than 1000 m² g⁻¹) but relatively small sphere diameters (less than 0.9 μm) and mean pore sizes (less than 2.2 nm).¹³ Considering that very low ammonia and CTAB concentrations were used in the current synthesis, which might provide less driving force for ordering, it is not unexpected that microspheres with disordered mesopores were obtained. Compared with ethanol, methanol may show much less inhibition effect on the development of long-range order, favoring the formation of silica spheres with hexagonally ordered mesopores; however, it may be reminded that methanol is a rather toxic solvent, which could limit its large scale application.

When the water-to-ethanol ratio was increased to 0.95, gigantic bowl-like hollow shells about 10–25 μm in diameter together with lots of small microspheres ~1.1 μm in diameter, which are similar to the pure mesoporous microspheres obtained at $r = 0.63$, were obtained (Figure 1c). The bowl-like hollow shells can be enriched by repeated sedimentation, and the high-magnification SEM image shown in Figure 1d suggests that the gigantic bowl-like structures are actually hollow shells consisting of an inner layer composed of many small spheres (typically 0.5–0.8 μm in diameter) and an outer thin layer (about 0.2–0.3 μm in thickness). These gigantic hollow structures composed of small silica spheres show an intriguing morphology mimicking the hierarchical structure of biogenetic silica in diatoms in a way. They are also reminiscent of the gigantic hollow silica spheres composed of primary mesoporous silica spheres prepared from EO₇₆PO₂₉EO₇₆/butanol/ethanol/water quaternary system, which did not, however, show an outer thin layer.²²

(33) Stöber, W.; Fink, A. *J. Colloid Interface Sci.* **1968**, *26*, 62.

(34) Wells, J. D.; Koopal, L. K.; de Keizer, A. *Colloids Surf., A* **2000**, *166*, 171.

(35) (a) Kruk, M.; Jaroniec, M.; Sayari, A. *Langmuir* **1997**, *13*, 6267. (b) Kruk, M.; Jaroniec, M. *Chem. Mater.* **2001**, *13*, 3169.

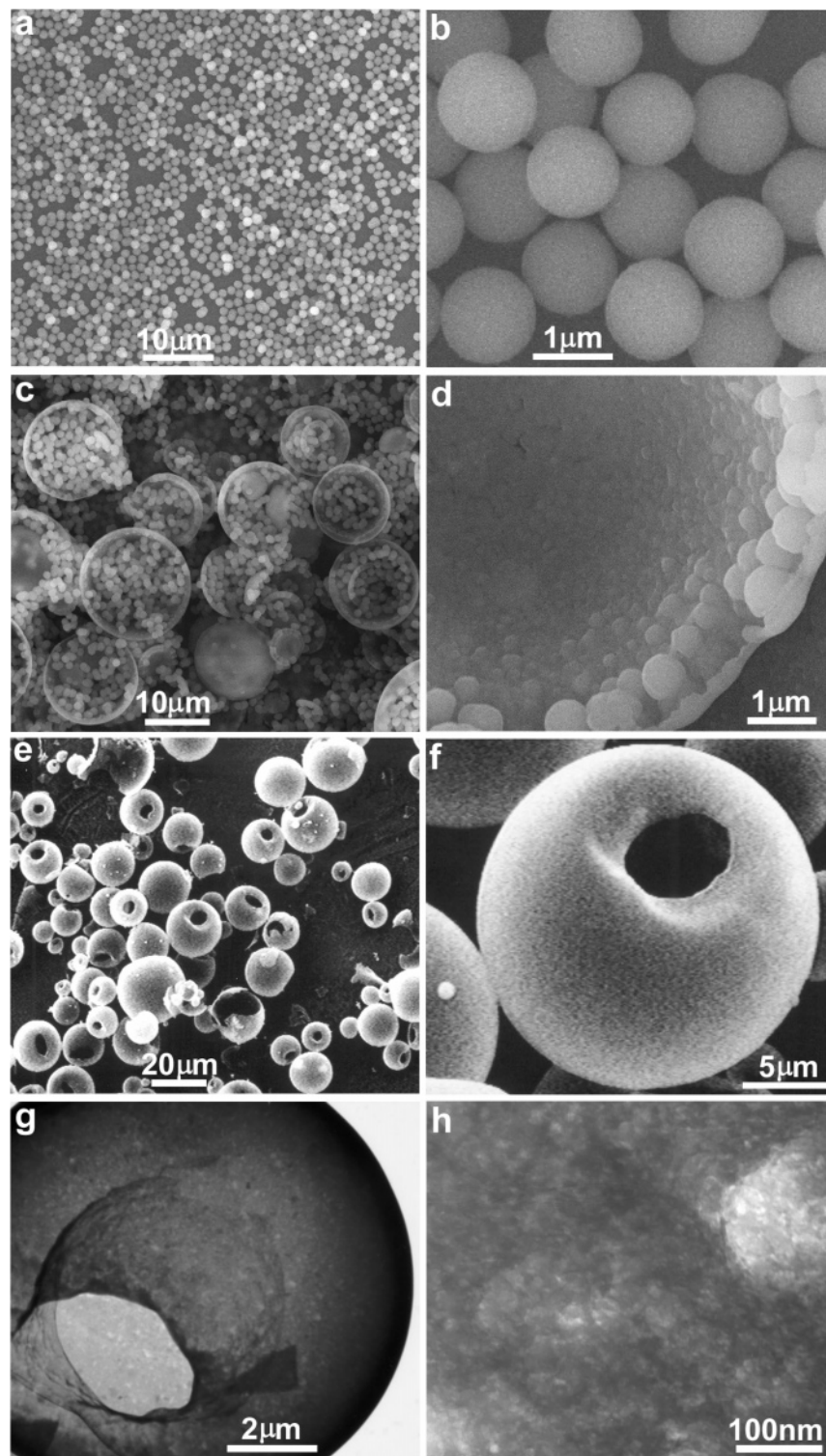


Figure 1. SEM (a–f) and TEM (g,h) images of mesoporous silica synthesized at different water-to-ethanol volume ratios (r): (a,b) monodisperse microspheres obtained at $r = 0.63$; (c,d) a mixture of microspheres and gigantic hollow shells composed of small spheres obtained at $r = 0.95$; (e–h) gigantic hollow shells obtained at $r = 1.44$. [CTAB] = 4.8 mM, TEOS volume content $x = 0.07$.

If the water-to-ethanol ratio was further increased to 1.44, gigantic hollow structures typically ranging from 5 to 25 μm in diameter, which showed a thin smooth shell with a single hole in general, became the predominant product (Figure 1e,f). The thickness of the shell was estimated to be around 100 nm from the TEM image shown in Figure 1g. A high-magnification TEM image is shown in Figure 1h, which suggests that there are many disordered mesopores with sizes less than 8 nm in the shell. The small-angle XRD pattern of the gigantic hollow shells exhibits

a broad peak corresponding to a d spacing of ~ 4.8 nm (Figure S1b, Supporting Information), indicating the presence of disordered mesopores in the shell, in agreement with the TEM observation. The nitrogen adsorption–desorption isotherms of the silica shells are basically of type IV and display a relatively small hysteresis loop (Figure 2b), confirming the presence of disordered mesopores. These hollow silica shells show a BET surface area of $655 \text{ m}^2 \text{ g}^{-1}$ and a pore volume of $0.653 \text{ cm}^3 \text{ g}^{-1}$, which are both larger than those for the monodisperse micro-

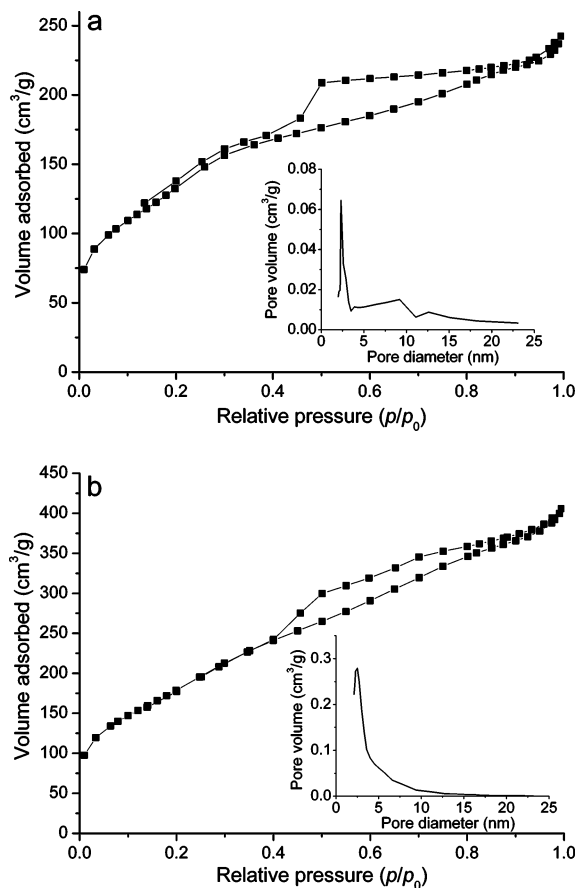


Figure 2. Nitrogen adsorption–desorption isotherms of mesoporous silica: (a) monodisperse microspheres obtained at $r = 0.63$; (b) gigantic hollow shells obtained at $r = 1.44$. Insets show the pore size distribution determined from the adsorption branch. [CTAB] = 4.8 mM, $x = 0.07$.

spheres obtained at $r = 0.63$. The pore size distribution determined from the adsorption branch shows a peak at 2.4 nm, and the average pore size was calculated to be 3.8 nm. To summarize, the morphology of mesoporous silica can be regulated from monodisperse microspheres through gigantic bowl-like hollow structures composed of small spheres to gigantic hollow structures with a smooth shell by simply increasing the water-to-ethanol value, that is, by decreasing the ethanol content in the solution. This result may be rationalized by considering that ethanol can decrease the immiscibility between TEOS and water, and hence a low ethanol content would favor the formation of an oil (TEOS)-in-water (mixed water–ethanol solution) emulsion, which could act as a template for the formation of the hollow silica shells. It can be noted that, while ordered mesoporous silica spheres were obtained previously in the same water–alcohol–ammonia–TEOS–CTAB system, hollow structures of mesoporous silica were not observed.^{6,36} The obtaining of hollow structures of mesoporous silica in the current synthesis might be largely attributed to the fact that the ammonia/TEOS ratio used here is very low, and the CTAB/TEOS ratio is extremely low, which could contribute to the formation of emulsion templates and lead to the lack of long-range order in the obtained mesoporous silica products.

Effect of the TEOS Volume Content (x). The effect of the TEOS content on the morphology of the mesoporous silica

products has been investigated at a fixed water-to-ethanol volume ratio ($r = 0.95$) and CTAB concentration (4.8 mM). As shown in Figure 3a, mesoporous silica microspheres with an average size of 1.15 μm (standard deviation $\sim 5.6\%$) were obtained at a relatively small x value ($x = 0.04$). Compared with the monodisperse microspheres obtained at $x = 0.07$ (Figure 1a), the monodispersity of these microspheres decreases slightly, and the presence of some dimers due to coagulation between the spheres is evident. As described above, a mixture of microspheres and gigantic bowl-like hollow shells composed of small spheres were produced when the x value was increased to 0.07. When the x value was further increased to $x = 0.14$, pure bowl-like half-shells with sizes of about 5–20 μm were obtained (Figure 3b). Close SEM and TEM observations suggest that the half-shells have relatively smooth outer and inner surfaces with a shell thickness of ~ 100 nm (Figure 3c,d). The nitrogen adsorption–desorption isotherms of the silica half shells are basically of type IV with a small hysteresis loop (Figure S2, Supporting Information), indicating the presence of disordered mesopores. These silica half shells show a BET surface area of 552 $\text{m}^2 \text{g}^{-1}$ and a pore volume of 0.308 $\text{cm}^3 \text{g}^{-1}$. The average pore size was estimated to be 3.3 nm from the adsorption–desorption isotherms. In short, the morphology of the mesoporous silica can be adjusted from uniform microspheres through gigantic bowl-like hollow shells composed of small spheres to gigantic half shells by simply increasing the TEOS content, that is, by increasing the amount of oil (TEOS) phase in the water phase (mixed water–ethanol solution).

Effect of the CTAB Concentration. Since the surfactant CTAB played the role of both the template for generating mesopores and the interfacial stabilizer for stabilizing the emulsion droplets, it is expected that the CTAB concentration would also affect the formation of emulsion and thus the final morphology of mesoporous silica. Figure 4 shows typical SEM images of the mesoporous silica products obtained at different CTAB concentrations when the water-to-ethanol volume ratio and the TEOS content are fixed at 0.95 and 0.07, respectively. At a relatively high CTAB concentration (13.3 mM), silica microspheres about 1.4–2.1 μm in diameter were obtained in addition to a small amount of gigantic bowl-like hollow shells composed of small spheres (Figure 4a). As described above, a mixture of microspheres and gigantic bowl-like hollow shells composed of small spheres were produced when the CTAB concentration was decreased to 4.8 mM. If the CTAB concentration was further decreased to 1.9 mM, gigantic hollow shells (about 2–20 μm in diameter) with a thin shell (~ 200 nm in thickness) were produced just as expected. Interestingly, gigantic hollow silica capsules like collapsed spherical shells with many folds and creases were obtained when the CTAB concentration was still further decreased to 0.95 mM (Figure 4c). The high-magnification image shown in Figure 4d suggests that the flexible shell has a thickness about 20–30 nm, much thinner than the thickness of the gigantic hollow shells obtained at a CTAB concentration of 1.9 mM. If the CTAB concentration was further decreased, the amount of precipitated silica products decreased significantly, and no precipitates were obtained when the CTAB concentration was decreased to below 0.5 mM, indicating that the CTAB molecules partitioning at the TEOS–water interface promoted the hydrolysis and condensation of TEOS at the oil–water interface of the oil (TEOS)-in-water emulsion.¹⁸

Formation Mechanism. The formation of the gigantic hollow shells of mesoporous silica shown in Figure 1e was monitored by examining samples taken at different time intervals using OM through a typical transmission light method (Figure 5). As

(36) Liu, S. Q.; Cool, P.; Collart, O.; van der Voort, P.; Vansant, E. F.; Lebedev, O. I.; van Tendeloo, G.; Jiang, M. H. *J. Phys. Chem. B* **2003**, *107*, 10405.

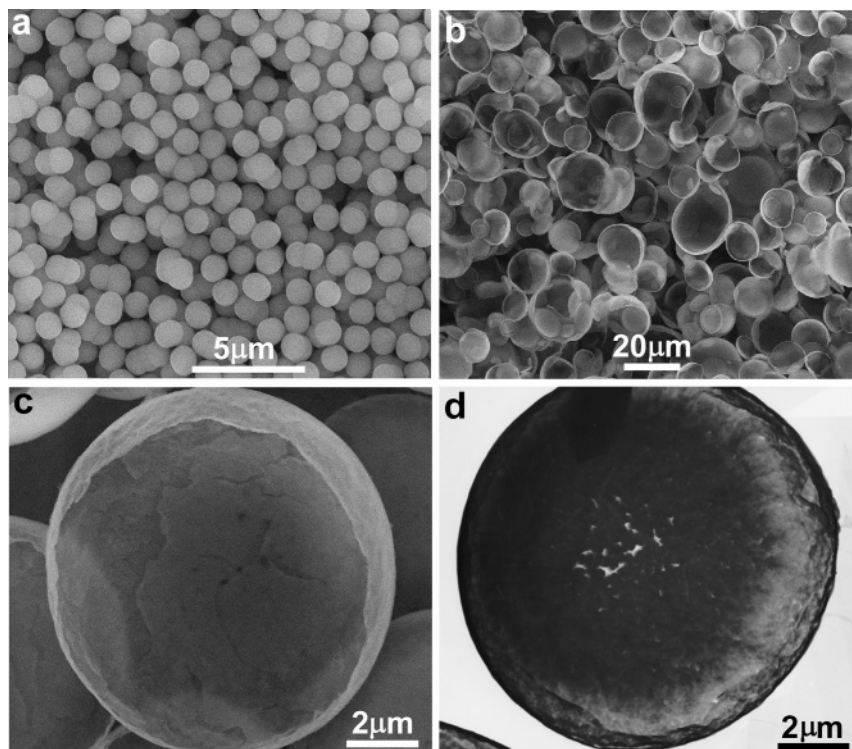


Figure 3. SEM (a–c) and TEM (d) images of mesoporous silica synthesized at different TEOS volume contents (x): (a) monodisperse microspheres obtained at $x = 0.04$; (b–d) bowl-like half shells obtained at $x = 0.14$. [CTAB] = 4.8 mM, $r = 0.95$.

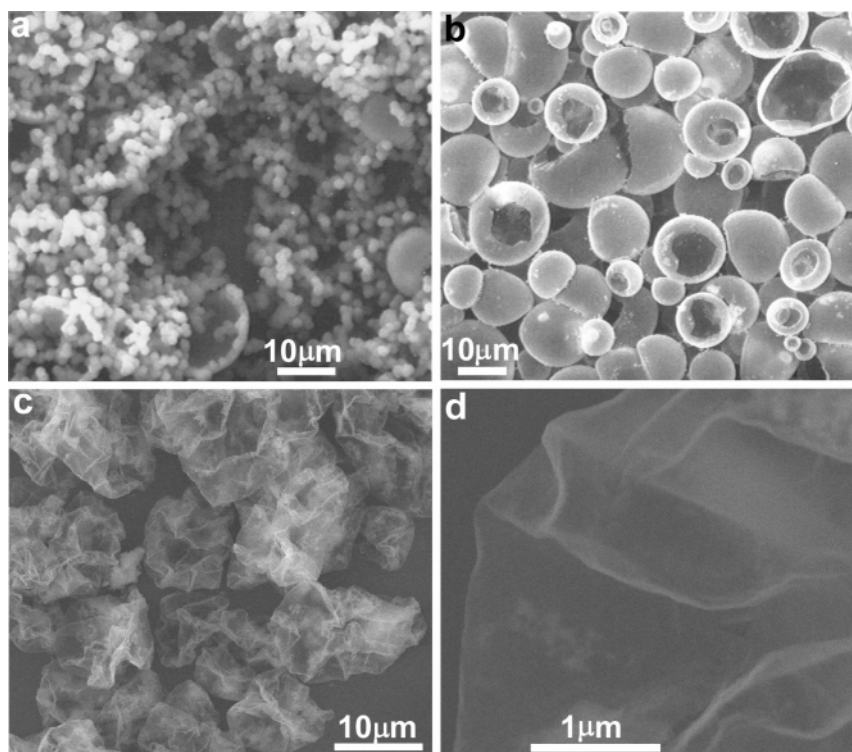


Figure 4. SEM images of mesoporous silica synthesized at different CTAB concentrations: (a) microspheres together with a few gigantic hollow shells obtained at [CTAB] = 13.3 mM; (b) gigantic hollow shells obtained at [CTAB] = 1.9 mM; (c,d) gigantic hollow capsules obtained at [CTAB] = 0.95 mM. $r = 0.95$, $x = 0.07$.

shown in Figure 5a, emulsion droplets about 5–25 μm in diameter formed immediately after mixing the solution with stirring. After 30 min of reaction, some gigantic hollow shells with similar sizes and a relatively large opening on the shell formed (Figure 5b). When the reaction time was prolonged to 3 h, many gigantic hollow shells with similar sizes and a relatively smaller opening

or hole on the shell were produced (Figure 5c). This result demonstrates that the gigantic hollow shells indeed formed by templating the emulsion droplets. It is also indicated that the hole on the shell of each hollow shell formed during the reaction process in the solution rather than during the drying or heat treatment process. These holes or openings could provide a

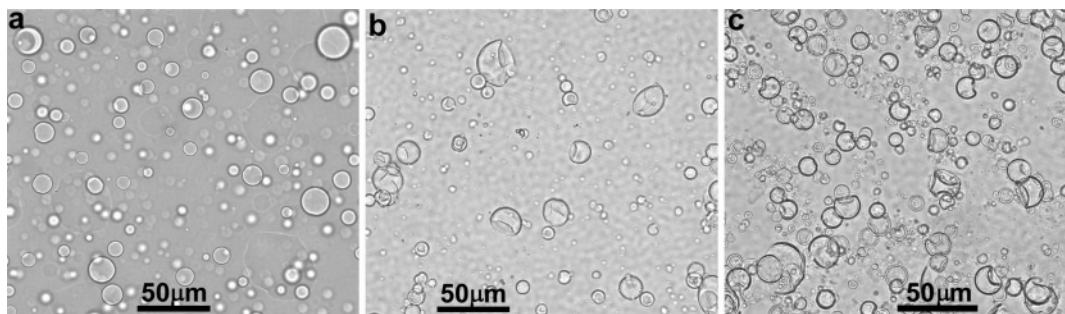


Figure 5. Optical micrographs of gigantic hollow shells of mesoporous silica obtained after different times of reaction: (a) 0 min; (b) 30 min; (c) 3 h. [CTAB] = 4.8 mM, $r = 1.44$, $x = 0.07$.

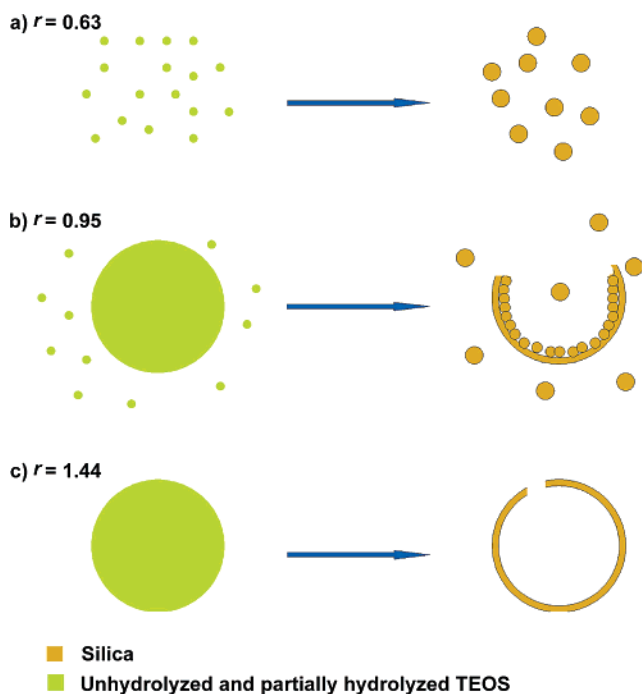


Figure 6. Schematic illustration of the morphology-controlled formation of mesoporous silica by adjusting the r values.

pathway for the unhydrolyzed TEOS inside the droplets flowing outside to undergo hydrolysis and condensation processes that mainly occurred at the oil–water interface of the emulsion droplets. Meanwhile, the surfactant molecules enriched at the oil–water interface could participate in the hydrolysis and condensation of TEOS, leading to the formation of the hollow mesoporous silica shells.

According to the above experimental results, it may be reasonably inferred that the existing state of the unhydrolyzed and partially hydrolyzed TEOS in the present water–ethanol–ammonia–TEOS–CTAB system (e.g., soluble or solubilized species and emulsion droplets) could play a key role in determining the morphology of the final mesoporous silica products. In particular, a tentative mechanism is proposed for the formation of the mesoporous silica with varied morphologies at different water-to-ethanol volume ratios (Figure 6). At a relatively low r ratio ($r = 0.63$), the relatively high ethanol content led to an enhanced solubility of TEOS in the solution. The unhydrolyzed and partially hydrolyzed TEOS existed exclusively as soluble species in the solution or solubilized species in the CTAB micelles, resulting in the formation of pure monodisperse mesoporous silica spheres. When the r ratio was increased to 0.95, the solubility of TEOS in the solution was considerably decreased. Large TEOS-in-water emulsion droplets coexisted

with the soluble and solubilized TEOS species, resulting in the formation of a mixture of the normal mesoporous silica microspheres and gigantic bowl-like hollow shells with hierarchical structures. The gigantic hollow structures consisting of an outer thin layer and an inner layer composed of small spheres could result from the initial hydrolysis and condensation of TEOS at the interface of the emulsion droplets to form a thin silica shell, which was followed by the formation and deposition of small silica spheres onto the inner surface of the thin shell gradually. When the r ratio was further increased to 1.44, the miscibility between TEOS and the mixed water–ethanol solution with a low ethanol content was dramatically decreased. The unhydrolyzed and partially hydrolyzed TEOS existed predominantly as large emulsion droplets in the solution, resulting in the formation of the gigantic hollow shells of mesoporous silica. A noticeable hole would form at one end of the shell as a channel for the outward diffusion of the TEOS droplet. Such a mechanism may be reasonably extended to explain the morphological control of mesoporous silica through adjusting the TEOS volume content and the CTAB concentration, considering that a higher TEOS content would favor the formation of a TEOS-in-water emulsion, while a higher CTAB concentration would favor the solubilization of TEOS as well as accelerate the hydrolysis of TEOS to form soluble TEOS species. Therefore, a plausible mechanism for the morphological regulation of mesoporous silica by adjusting various experimental parameters emerges. Namely, the morphology of mesoporous silica can be regulated from microspheres through gigantic hollow shells composed of small spheres to gigantic hollow structures with a thin shell by simply adjusting the existing state of the unhydrolyzed and partially hydrolyzed TEOS in the solution through increasing the water-to-ethanol volume ratio, increasing the TEOS volume content, or decreasing the CTAB concentration. It has been made clear that emulsion-mediated silica synthesis is a promising biomimetic approach in studying the biosilicification mechanisms that lead to controlled nanostructures of silica.⁴ The present synthesis of mesoporous silica with various morphologies, such as the well-defined hollow shells somewhat resembling the biogenic silica exoskeleton in diatoms, would help one understand or explain processes underlying diatom biosilica formation.

Conclusions

It has been demonstrated that the morphosynthesis of mesoporous silica with a variety of morphologies, such as monodisperse microspheres, gigantic hollow structures comprising a thin shell with a hole, and gigantic bowl-like hollow structures composed of small spheres, can be readily realized in the water–ethanol–ammonia–TEOS–CTAB system. Generally, the morphology of mesoporous silica can be regulated from microspheres through gigantic hollow shells composed of small spheres to gigantic hollow structures with a thin shell by increasing the water-to-

ethanol volume ratio, increasing the TEOS volume content, or decreasing the CTAB concentration. A plausible mechanism for the morphological regulation of mesoporous silica by adjusting various experimental parameters has been put forward by considering the existing state of the unhydrolyzed and partially hydrolyzed TEOS in the synthesis system (e.g., soluble or solubilized species and emulsion droplets). While monodisperse microspheres were obtained when the unhydrolyzed and partially hydrolyzed TEOS existed exclusively as soluble or solubilized species, gigantic hollow shells were produced when the unhydrolyzed and partially hydrolyzed TEOS existed predominantly as emulsion droplets that acted as templates for the formation of hollow shells. The facile synthesis of mesoporous silica with well-defined morphologies and hierarchical structures at room temperature is reminiscent of the intriguing biosilicification

process in diatoms. The obtained mesoporous silica materials with various morphologies may find potential applications in fields including catalysis, separation, and photonic crystals.

Acknowledgment. This work was supported by the National Natural Science Foundation of China (20325312, 20473003, 50521201, and 20233010) and the Foundation for the Author of National Excellent Doctoral Dissertation of China (200020).

Supporting Information Available: XRD patterns of monodisperse microspheres obtained at $r = 0.63$ and gigantic hollow shells obtained at $r = 1.44$. This material is available free of charge via the Internet at <http://pubs.acs.org>.

LA062542L

Facile Synthesis of Monodisperse Microspheres and Gigantic Hollow Shells of Mesoporous Silica in Mixed Water-Ethanol Solvents

Huijuan Zhang, Jun Wu, Longping Zhou, Dayong Zhang, and Limin Qi*

Beijing National Laboratory for Molecular Sciences (BNLMS), State Key Laboratory for Structural Chemistry of Unstable and Stable Species, College of Chemistry, Peking University, Beijing 100871, P. R. China. E-mail: liminqi@pku.edu.cn

Supporting Information

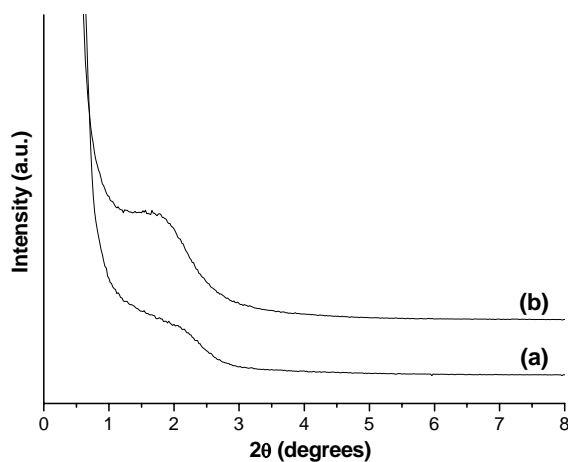


Figure S1. XRD patterns of mesoporous silica: (a) monodisperse microspheres obtained at $r = 0.63$; (b) gigantic hollow shells obtained at $r = 1.44$. [CTAB] = 4.8 mM, $x = 0.07$.

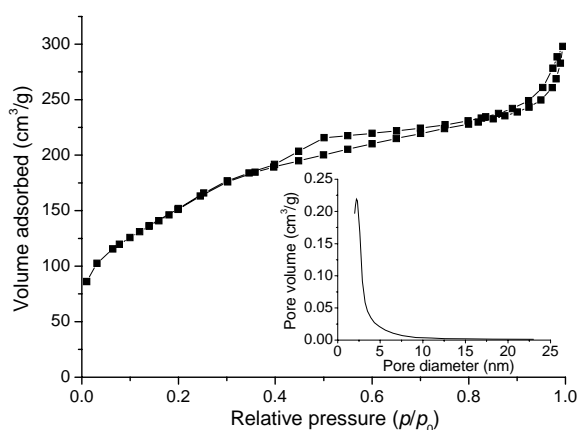


Figure S2. Nitrogen adsorption-desorption isotherms of bowl-like half shells of mesoporous silica obtained at $x = 0.14$. Inset shows the pore size distribution determined from the adsorption branch. [CTAB] = 4.8 mM, $r = 0.95$.